Acta Crystallographica Section F
Structural Biology and Crystallization Communications
ISSN 1744-3091

Cocrystallizing natural RNA with its unnatural mirror image: biochemical and preliminary X-ray diffraction analysis of a 5S rRNA A-helix racemate

Charlotte Förster,[a] Arnd B. E. Brauer,[a] Daniel Lehmann,[a] Tordis Borowski,[a] Svenja Brode,[a]‡ Jens P. Fürste,[a] Markus Perbandt,[b] Christian Betzel[b] and Volker A. Erdmann[a]*

[a]Institute of Chemistry and Biochemistry, Free University Berlin, Thielallee 63, 14195 Berlin, Germany, and [b]Institute of Biochemistry and Molecular Biology, University of Hamburg, c/o DESY, Notkestrasse 85, Building 22a, 22603 Hamburg, Germany

‡ Current address: Proteros Biostructures GmbH, Am Klopferspitz 19, 82152 Martinsried, Germany.

Correspondence e-mail: erdmann@chemie.fu-berlin.de

Received 25 July 2007
Accepted 18 August 2007

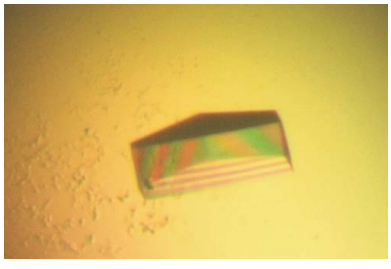

Chemically synthesized RNAs with the unnatural L-configuration possess enhanced *in vivo* stability and nuclease resistance, which is a highly desirable property for pharmacological applications. For a structural comparison, both L- and D-RNA oligonucleotides of a shortened *Thermus flavus* 5S rRNA A-helix were chemically synthesized. The enantiomeric RNA duplexes were stochiometrically cocrystallized as a racemate, which enabled analysis of the D- and L-RNA enantiomers in the same crystals. In addition to a biochemical investigation, diffraction data were collected to 3.0 Å resolution using synchrotron radiation. The crystals belonged to space group $P3_121$, with unit-cell parameters $a = b = 35.59$, $c = 135.30$ Å, $\gamma = 120^\circ$ and two molecules per asymmetric unit.

1. Introduction

The development of RNA 'spiegelmers' (Klussmann *et al.*, 1996; Nolte *et al.*, 1996) has led to new approaches in biochemistry as well as in diagnostic and therapeutic medicine. 'Spiegelmers' are 'mirror-image' RNA aptamers in the L-configuration, which exhibit enhanced stability and nuclease resistance (Klussmann *et al.*, 1996; Nolte *et al.*, 1996) compared with the natural D-RNA configuration (Fig. 1). Using the SELEX method (Ellington & Szostak, 1990; Tuerk & Gold, 1990), such RNA aptamers can be developed against almost any target, which they can bind with high affinity and high specificity. The biological function of an aptamer is similar to that of an antibody.

We are particularly interested in determining the L- and D-RNA structures in a comparative way in order to analyze their differing biochemical properties. Thereby, the as yet unanswered question why nature has favoured one enantiomer over the other during evolution will also be addressed.

To date, only one enantiomeric RNA system has been investigated by X-ray crystallography. This was derived from the 5S rRNA 8-mer

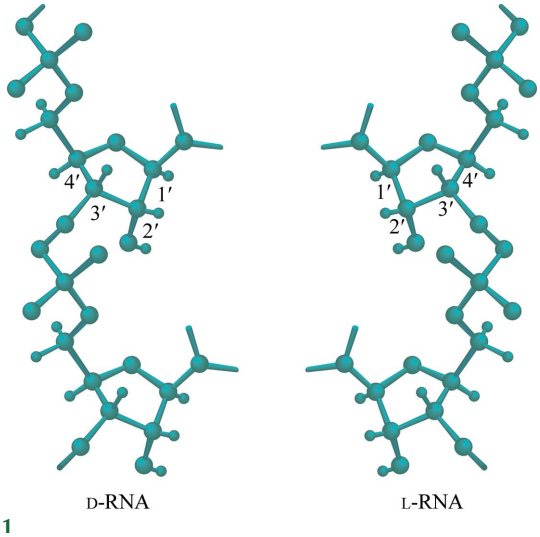

Figure 1
Schematic representation of the phosphate-sugar backbone of D- and L-RNA enantiomers. The chiral sugar-ring C atoms are labelled according to standard nomenclature.

E-helix of *Thermus flavus* (Fig. 2). The X-ray structures of a 5S rRNA 8-mer E-helix were solved to high resolution in the D-form (Perbandt *et al.*, 2001) and in the L-form (Vallazza *et al.*, 2004). Attempts to crystallize the L-enantiomer under the same or similar conditions as the D-enantiomer unexpectedly failed. The successful crystallization conditions for the L-enantiomer, which led to crystals that were suitable for X-ray diffraction and that diffracted well (Vallazza *et al.*, 2004), differed from those for the natural RNA with the D-configuration (Perbandt *et al.*, 2001). The different crystallization environment may also be reflected in the main observed structural differences, namely the respective absence and presence of a wobble-like G·C base pair and the altered hydration pattern within the setting of an A-type helix (Vallazza *et al.*, 2004). An elegant way to harmonize the crystallization conditions is the stochiometric cocrystallization of the D- and L-enantiomers as successfully performed for the 5S rRNA E-helix racemate (Rypniewski *et al.*, 2006). This racemate structure was solved to high resolution, showing a complex arrangement of the constituent helices, all of which adopt an A-type conformation that is mirrored between the enantiomers (Rypniewski *et al.*, 2006). In order to explore the variability of the geometric arrangement of the enantiomeric duplexes as well as the (dis)similarities between the enantiomers, we here report the analysis of a second related system. A shortened *T. flavus* 7-mer 5S rRNA A-helix (Fig. 2), the structure of which has been solved in a dodecamer

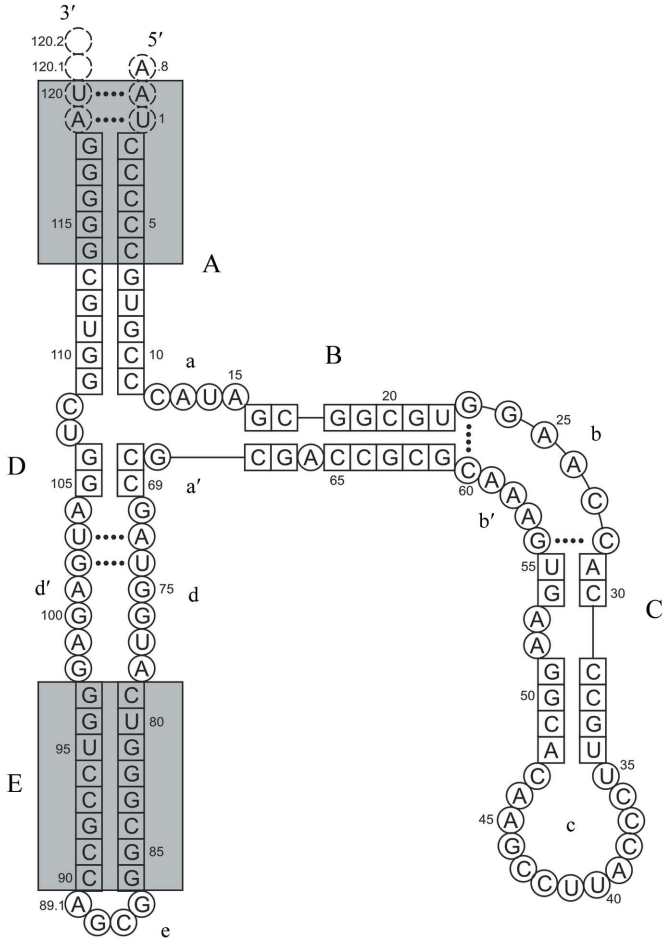

Figure 2
Secondary structure of *T. flavus* 5S rRNA. The letters A–E indicate the single domains of 5S rRNAs. The 7-mer oligonucleotide part of the A-helix, which is examined in this study, and the 8-mer oligonucleotide part of the E-helix are highlighted by boxes.

D-RNA to 2.4 Å resolution (Betzel *et al.*, 1994), was chemically synthesized in both enantiomeric forms. These were cocrystallized as a racemate and examined biochemically.

2. Materials and methods

2.1. RNA synthesis

The RNA oligomers were synthesized on an Applied Biosystems 394 DNA/RNA synthesizer by solid-phase phosphoramidite chemistry with the following D-RNA phosphoramidites: 5′-DMT-2′-tBDMS-rA(bz)-3′-CEP, 5′-DMT-2′-tBDMS-rG(ib)-3′-CEP, 5′-DMT-2′-tBDMS-rC(bz)-3′-CEP and 5′-DMT-2′-tBDMS-rU-3′-CEP [from Proligo, ChemGenes or by own synthesis; DMT, dimethyltrityl-; tBDMS, (*tert*-butyl)-dimethylsilyl-; bz, benzoyl; ib, isobutyryl; CEP, cyanoethyl-*N*,*N*-diisopropyl-phosphoramidite]. The corresponding L-RNA phosphoramidites were synthesized in-house as reported by Nolte *et al.* (1996).

The synthesis was performed on the 1 µmol scale using the DMT-on strategy on ChemGenes or Proligo CPG 500A columns. Following synthesis, the RNA was deprotected with 40% aqueous methylamine for 20 min at 338 K. RNA strands were then lyophilized. The oligonucleotides were resuspended in 150 µl dimethyl sulfoxide (DMSO), 75 µl triethanolamine (TEA) and 200 µl 37% TEA in HF for 2 h at 338 K. A 10 ml reverse-phase column from Amersham Biosciences (15 RPC) was used for purification of the DMT-on product. The lyophilized DMT-on fractions were resuspended in 50 µl 80% acetic acid and incubated for 1 h at 323 K to remove the DMT group. After adjusting the pH to 6.5 with 3 *M* sodium acetate, the RNA was purified again by HPLC chromatography as described above and was further desalted using G-10 columns (Pharmacia, Uppsala, Sweden). Analytical HPLC was applied to analyze the purity of the RNA product using the following buffer system: buffer *A*, 50 m*M* TEA acetate pH 7.0; buffer *B*, 80% acetonitrile in 50 m*M* TEA acetate pH 7.0. The UV-absorption method of Sproat *et al.* (1995) was used to quantify the RNA product.

2.2. RNA hybridization

The hybridization of the two complementary strands of the *T. flavus* 5S rRNA 7-mer A-helix, 5′-GGGGGAU-3′ and 5′-AUCCCCC-3′ (Fig. 2), was performed in water at a concentration of 0.5 m*M* each. This was performed independently for the complementary D-RNA strands and the complementary L-RNA strands. After heating to 363 K, the RNAs were cooled to room temperature over several hours. Stochiometric amounts of the resulting D- and L-RNA duplexes were combined to a final concentration of 0.5 m*M* RNA duplexes in total (*i.e.* consisting of 0.25 m*M* D- and L-RNA duplex concentration each). This D-RNA and L-RNA racemate mixture was used for the following biochemical and crystallization experiments.

2.3. Crystallization of the 5S rRNA A-helix as D- and L-RNA racemate

To avoid degradation of the RNAs by RNases, the following precautions were taken: glass tubes were either cleaned with chromesulfuric acid or heated to 448 K for 4 h prior to usage. Water was treated with 0.1%(*w*/*v*) diethylpyrocarbonate. No special treatment could be applied to plastic tubes or special screening solutions other than autoclaving or sterile filtration. Rather fast crystallization is an advantage in avoiding RNA degradation. No solutions with pH values above 7.0 were used for crystallization screening owing to the

susceptability of RNA to alkaline hydrolysis. The integrity of the RNAs was examined by mass spectrometry (data not shown) or polyacrylamide gel electrophoresis.

Initial crystallization screening experiments were performed applying the Natrix Formulation and the Nucleic Acid Mini Screen from Hampton Research (CA, USA). Using the sitting-drop vapour-diffusion technique, 1 µl samples of RNA in H_2O were mixed with 1 µl reservoir solution and equilibrated against 80 µl reservoir solution at 294 K in CrystalQuick Lp Plates (Greiner Bio-One, Germany). Small crystals with hexagonal morphology appeared after 3–4 d with crystallization solutions containing lithium sulfate as precipitant. Conditions were optimized to the following final solutions: 0.05 *M* HEPES–NaOH pH 7.0, 0.05 *M* magnesium sulfate and 1.7 *M* lithium sulfate. Subsequently, crystals were grown using the hanging-drop vapour-diffusion technique. 1 µl 0.5 m*M* RNA racemate solution was mixed with 1 µl reservoir solution and equilibrated against 1 ml reservoir solution in 24-well Linbro Plates (ICN Biomedicals Inc., Ohio, USA) at 294 K. Crystals appeared after 2 d with approximate dimensions of 0.25 × 0.25 × 0.15 mm.

2.4. Polyacrylamide gel electrophoresis and RNase digestion of D- and L-RNAs

RNA oligonucleotides were separated by gel electrophoresis on gels containing 20%(*w*/*v*) polyacrylamide, 0.55%(*w*/*v*) *N*,*N*′-methylene bisacrylamide, 89 m*M* Tris, 89 m*M* boric acid, 2.5 m*M* EDTA, 0.1%(*w*/*v*) TEMED and 7 *M* urea. 150 pmol of RNA or nuclease digests of RNA (described below) were applied onto the gel. Prior to gel loading, the RNA or RNA digests were heated to 363 K, immediately cooled on ice and mixed with 7 *M* urea and 30%(*v*/*v*) glycerol. To avoid interference of the short oligonucleotide RNAs with the migration of gel colour markers during electrophoresis, the following loading buffer was applied beside the RNA-sample lanes: 5 m*M* Tris, 5 m*M* boric acid, 1 m*M* EDTA, 30% sucrose, 0.02%(*w*/*v*) xylencyanol and 0.02%(*w*/*v*) bromophenol blue. Electrophoresis was performed at 650 V with 89 m*M* Tris, 89 m*M* boric acid, 2.5 m*M* EDTA as electrophoresis buffer.

RNA was detected by staining with 'Stains-All' (Fluka/Sigma–Aldrich, Taufkirchen, Germany); the solution contained 0.005%(*w*/*v*) 'Stains-All' in 50%(*v*/*v*) aqueous formamide. Staining was performed for 1 h in the dark prior to destaining with H_2O for several hours in light. Following documentation of the 'Stains-All' result, silver staining was applied to increase the sensitivity of RNA visualization on the gel. 'Roti-Black N' nucleic acid silver-staining reagents were supplied by Roth (Karlsruhe, Germany) and were used as described by the manufacturer's product sheet. Documentation and quantification of the gels was performed using the Gel Doc 2000 system (BioRad, Munich, Germany).

For complete RNA digestion, two alternative procedures were used. Following the generation of single-stranded RNA by heating the RNA 7-mer duplexes to 363 K and subsequent instant cooling on ice, nuclease S1 digestion of D-RNA, L-RNA and the RNA racemate took place using the enzyme from *Aspergillus oryzae* (10 U µl^{-1}; Fermentas, St Leon-Rot, Germany). 150 pmol RNA was incubated with 100 U nuclease S1 in the following reaction buffer: 40 m*M* sodium acetate pH 4.5, 300 m*M* sodium chloride, 2 m*M* zinc sulfate at 310 K for 20 min.

In an additional experiment, a mixture of RNase T1 and RNase V1 was used without prior generation of single-stranded RNA. *Escherichia coli* RNase T1 with a specific activity of 100 U µl^{-1} was purchased from Fermentas (St Leon-Rot, Germany). Snake-venom phosphodiesterase V1 with an activity of 10 U µl^{-1} from cobra venom was supplied by Ambion (Darmstadt, Germany). The RNA was digested with a mixture of RNAse T1 and RNAse V1 with 1 U µl^{-1} using the following reaction conditions: 50 m*M* Tris–HCl pH 7.5, 310 K, 20 min reaction time.

2.5. Crystallographic data collection and evaluation

Prior to data collection, the crystals were transferred into a cryoprotectant solution containing 0.05 *M* HEPES–NaOH pH 7.0, 0.05 *M* magnesium sulfate, 1.7 *M* lithium sulfate, 20%(*v*/*v*) glycerol and flash-frozen in liquid nitrogen. Several X-ray diffraction data sets were acquired on the X13 consortium beamline at the DESY synchrotron in Hamburg (DESY/HASYLAB, Hamburg, Germany) and on the X-ray diffraction beamline XRD1 at the Elettra synchrotron (Trieste, Italy). At the latter, the best data set obtained to date was recorded from 20.0 to 3.0 Å resolution using a wavelength of 1.0 Å at 100 K. The *HKL*-2000 package (Otwinowski & Minor, 1997) was used for data processing and determination of the space group and unit-cell parameters. The diffraction data were analysed for merohedral twinning using the algorithm of Padilla & Yeates (2003) as implemented in the web server http://nihserver.mbi.ucla.edu/pystats. Molecular-replacement calculations are in progress using the programs *AMoRe* (Navaza, 1994) and *Phaser* (McCoy *et al.*, 2005) within the *CCP4i* package (Collaborative Computational Project, Number 4, 1994).

3. Results and discussion

3.1. Crystallization

The initial screening for suitable conditions for cocrystallizing a stochiometric mixture of the D- and L-enantiomers of the *T. flavus* 5S rRNA 7-mer A-helix (Fig. 2) indicated lithium sulfate to be a particularly suitable precipitant. Building on this, the conditions were iteratively optimized to 0.05 *M* HEPES–NaOH pH 7.0, 0.05 *M* magnesium sulfate and 1.7 *M* lithium sulfate. Under these conditions, crystals with hexagonal morphology and approximate dimensions of 0.25 × 0.25 × 0.15 mm appeared after 2 d at 294 K (Fig. 3).

3.2. Biochemical experiments

In order to obtain evidence that the crystals consisted of a mixture of enantiomers, we made use of the fact that L-RNAs are not degraded enzymatically by RNase, in contrast to the natural D-RNAs. Owing to their RNase resistance, L-RNA enantiomers can still be detected by gel analysis after RNase S1 digestion, while the D-RNA

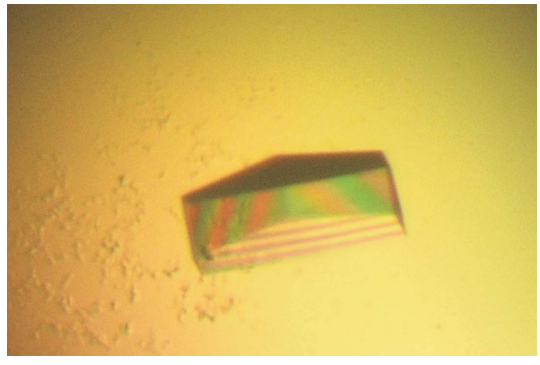

Figure 3
Crystal of *T. flavus* 5S rRNA 7-mer A-helix racemate with approximate dimensions of 0.25 × 0.25 × 0.15 mm.

enantiomers are rapidly degraded (Fig. 4*a*). Using detection with 'Stains-All', we could observe a slight difference in band migration and a difference in the colouration behaviour of the oligonucleotide single strands. The purine-rich strand is dark blue/purple and shows a slower migration than the pyrimidine-rich cyan-coloured strand. These features are independent of chirality. After RNase V1/T1 digestion of D-/L-RNA racemates approximately half of the RNA is degraded, which is assigned to the digestion of the D-RNA component (Figs. 4*b* and 4*c*): this holds true for the digestion of a pipetted racemic solution (DL-s) and for crystals that were dissolved in water (DL-c) after careful repeated washing with crystallization solution to avoid contamination with noncrystallized RNA from the crystallization droplet. These observations would be consistent with the cocrystallization of the D- and L-RNA enantiomers of the 5S rRNA A-helix. This in turn would be consistent with the rule of Wallach (Wallach, 1895; Brock *et al.*, 1991). However, caution should be taken with the quantification of the 'Stains-All' and silver-stained RNAs beyond the above trend analysis because of complications arising from intensity differences in staining purines and pyrimidines. In particular, silver staining produced a fast oversaturation of the purine-rich strands compared with the pyrimidine-rich strands.

3.3. Crystallographic data

Here, we report the X-ray diffraction data of the *T. flavus* 5S rRNA 7-mer A-helix racemate to 3.0 Å using synchrotron radiation at a wavelength of 1.0 Å and cryogenic cooling. The data were processed in the 20.0–3.0 Å resolution range with an overall $R_{\rm merge}$ of 5.3% and a completeness of 96.5% (Table 1). The *T. flavus* 7-mer A-helix racemate crystallizes in space group $P3_121$, with unit-cell parameters $a = b = 35.59$, $c = 135.30$ Å, $\gamma = 120.00^\circ$. Assuming the presence of two

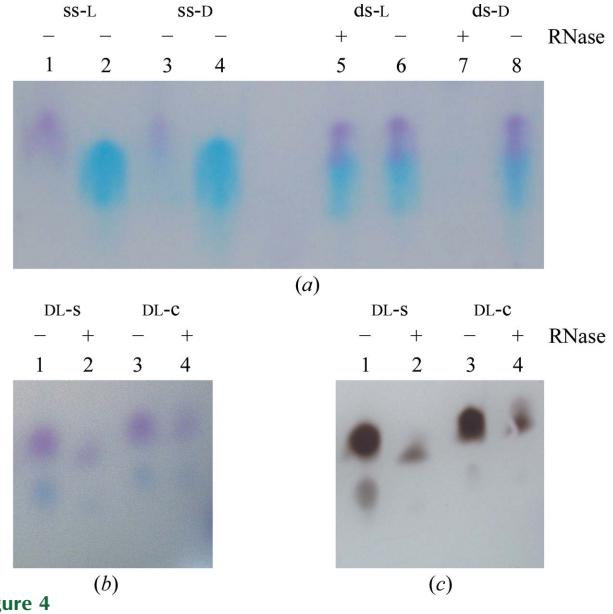

Figure 4
Polyacrylamide gel electrophoresis of the single-stranded (ss) and double-stranded (ds) L- and D-enantiomers as well as the racemic mixture (DL) derived from the 5S rRNA 7-mer A-helix before (−) and after (+) RNase digestion. DL-s and DL-c denote a racemic solution and crystals that have been washed and dissolved, respectively. (*a*) Lanes 1 and 3 and lanes 2 and 4 contain the purine-rich 5′-GGGGGAU-3′ and the pyrimidine-rich 5′-AUCCCCC-3′ single strands, respectively. Lanes 5 and 7 show RNase S1 treatment of the D- and L-RNA double strands and lanes 6 and 8 the control experiment without RNase S1. 'Stains-All' was used for detection. (*b*) and (*c*) RNAse V1/T1 racemate digest with initial 'Stains-All' detection used for a quantification estimate (*b*) followed by additional silver staining for higher sensitivity (*c*).

Table 1
Data-collection and processing statistics of the *T. flavus* 5S rRNA 7-mer A-helix racemate.

Values in parentheses are for the highest resolution shell.

Beamline	XRD1, Elettra
Wavelength (Å)	1.000
Space group	$P3_121$
Unit-cell parameters (Å, °)	$a = b = 35.59$, $c = 135.30$, $\gamma = 120.00$
Matthews coefficient $V_{\rm M}$ (Å^3 Da^{-1})	2.81
RNA duplexes per asymmetric unit	2
Solvent content† (%)	66
Measured reflections	11671
Unique reflections	2202
Resolution range (Å)	20.0–3.0 (3.05–3.00)
Completeness (%)	96.5 (94.4)
Multiplicity (%)	5.3 (4.8)
$R_{\rm merge}$‡ (%)	5.3 (7.8)
Average $I/\sigma(I)$	13.9 (3.2)

† Estimated with the average partial specific volume calculated for RNA by Voss & Gerstein (2005). ‡ $R_{\rm merge} = \sum_{hkl}\sum_i |I_i(hkl) - \langle I(hkl)\rangle| / \sum_{hkl}\sum_i I_i(hkl)$, where $I_i(hkl)$ and $\langle I(hkl)\rangle$ are the observed individual and mean intensities of a reflection with indices hkl, respectively, $\sum_i$ is the sum over the individual measurements of a reflection with indices hkl and $\sum_{hkl}$ is the sum over all reflections.

molecules in the asymmetric unit, we calculated a Matthews coefficient $V_{\rm M}$ (Matthews, 1968) of 2.81 Å^3 Da^{-1} and a corresponding water content of 66% using the parameters of Voss & Gerstein (2005). The diffraction data of the *T. flavus* A-helix racemate crystal were analyzed for merohedral twinning by applying the algorithm of Padilla & Yeates (2003). As the results correspond to the theoretical curve for an untwinned crystal, we have no indication of merohedral twinning (data not shown).

Solution of the structure of the 5S rRNA A-helix racemate will be attempted by molecular-replacement calculations. The initial models for the enantiomers will be based on fragments of *T. flavus* 5S rRNA, including the D-RNA A-helix (Betzel *et al.*, 1994; PDB code 353d), the D-RNA E-helix (Perbandt *et al.*, 2001; PDB code 439d), the L-RNA E-helix (Vallazza *et al.*, 2004; PDB code 1r3o) and the racemic E-helix enantiomers (Rypniewski *et al.*, 2006; PDB code 2g32). These different models, if not 7-mers, will be shortened to the length of the RNA racemates. For the structural comparison of D- and L-RNA enantiomers, it is advantageous to examine the crystal structure of a racemate because the enantiomeric RNAs are then crystallized under identical conditions, as demonstrated recently by the structure of the 5S rRNA E-helix racemate (Rypniewski *et al.*, 2006). As this structure exhibits a very complex arrangement of the enantiomeric constituents, a comparison with the A-helix 5S rRNA racemate structure would provide further information concerning both the geometric arrangement and the structural details of racemic RNA crystal structures. The question also arises why nature has favoured the D-RNA enantiomers in evolution. Are there energetic or structural differences between L- and D-RNA enantiomers or are they simply structural mirror-image RNAs? Owing to their RNase resistance, the synthetic L-RNAs, especially the 'spiegelmer' aptamers, provide a promising diagnostic and therapeutic tool. The comparative structure determination of L-RNA and D-RNA aims to broaden the experimental basis for the discussion of these issues.

This work was funded within the RiNA network for RNA technologies by the Federal Ministry of Education and Research, the City of Berlin and the European Regional Development Fund. We thank the Fonds der Chemischen Industrie (Verband der Chemischen Industrie e.V.) and National Foundation for Cancer Research, USA for additional support. We gratefully acknowledge the European

Union for reimbursement under the EU contract RII3-CT-2004-506008 (IA-SFS) and the Elettra synchrotron (Trieste, Italy) and the DESY synchrotron (Hamburg, Germany) for providing beamtime. We thank Diana Rothe and Chris Weise for excellent technical support and helpful discussions.

References

Betzel, C., Lozenz, S., Fürste, J. P., Bald, R., Zhang, M., Schneider, T. R., Wilson, K. S. & Erdmann, V. A. (1994). *FEBS Lett.* **351**, 159–164.
Brock, C. P., Schweizer, W. B. & Dunitz, J. D. (1991). *J. Am. Chem. Soc.* **113**, 9811–9820.
Collaborative Computational Project, Number 4 (1994). *Acta Cryst.* D**50**, 760–763.
Ellington, A. & Szostak, J. J. (1990). *Nature (London)*, **346**, 818–822.
Klussmann, S., Nolte, A., Bald, R., Erdmann, V. A. & Fürste, J. P. (1996). *Nature Biotechnol.* **14**, 1112–1115.
McCoy, A. J., Grosse-Kunstleve, R. W., Storoni, L. C. & Read, R. J. (2005). *Acta Cryst.* D**61**, 458–464.
Matthews, B. W. (1968). *J. Mol. Biol.* **33**, 491–497.
Navaza, J. (1994). *Acta Cryst.* A**50**, 157–163.
Nolte, A., Klussmann, S., Bald, R., Erdmann, V. A. & Fürste, J. P. (1996). *Nature Biotechnol.* **14**, 1116–1119.
Otwinowski, Z. & Minor, W. (1997). *Methods Enzymol.* **276**, 307–326.
Padilla, J. E. & Yeates, T. O. (2003). *Acta Cryst.* D**59**, 1124–1130.
Perbandt, M., Vallazza, M., Lippmann, C., Betzel, C. & Erdmann, V. A. (2001). *Acta Cryst.* D**57**, 219–224.
Rypniewski, W., Vallazza, M., Perbandt, M., Klussmann, S., DeLucas, L. J., Betzel, C. & Erdmann, V. A. (2006). *Acta Cryst.* D**62**, 659–664.
Sproat, B., Colonna, F., Mullah, B., Tsou, D., Andrus, A., Hampel, A. & Vinayak, R. (1995). *Nucleosides Nucleotides*, **14**, 255–273.
Tuerk, C. & Gold, L. (1990). *Science*, **249**, 505–510.
Vallazza, M., Perbandt, M., Klussmann, S., Rypniewski, W., Einspahr, H. M., Erdmann, V. A. & Betzel, Ch. (2004). *Acta Cryst.* D**60**, 1–7.
Voss, N. R. & Gerstein, M. (2005). *J. Mol. Biol.* **346**, 477–492.
Wallach, O. (1895). *Liebigs Ann. Chem.* **286**, 90–143.